Article

Hybrid QM/MM and DFT Investigations of the Catalytic Mechanism and Inhibition of the Dinuclear Zinc Metallo-β-Lactamase CcrA from *Bacteroides fragilis*

Hwangseo Park, Edward N. Brothers, and Kenneth M. Merz

J. Am. Chem. Soc., **2005**, 127 (12), 4232-4241• DOI: 10.1021/ja042607b • Publication Date (Web): 08 March 2005

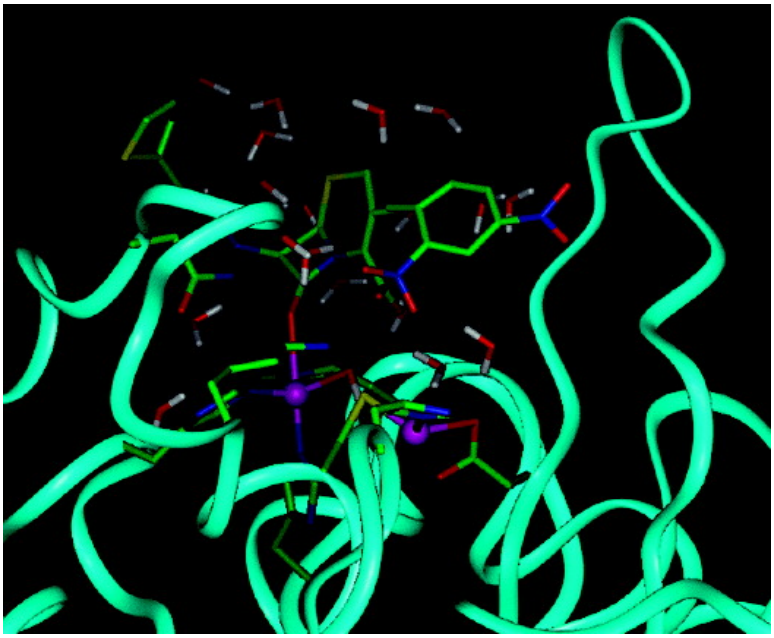

J|A|C|S
ARTICLES
Published on Web 03/08/2005

Hybrid QM/MM and DFT Investigations of the Catalytic Mechanism and Inhibition of the Dinuclear Zinc Metallo-β-Lactamase CcrA from *Bacteroides fragilis*

Hwangseo Park, Edward N. Brothers, and Kenneth M. Merz, Jr.*

Contribution from the Department of Chemistry, 104 Chemistry Building, Pennsylvania State University, University Park, Pennsylvania 16802-6300

Received December 9, 2004; E-mail: merz@psu.edu

Abstract: Based on hybrid QM/MM molecular dynamics simulation and density functional theoretical (DFT) calculations, we investigate the mechanistic and energetic features of the catalytic action of dizinc metallo-β-lactamase CcrA from *Bacteroides fragilis*. The 200 ps QM/MM simulation of the CcrA enzyme in complex with nitrocefin shows that the substrate β-lactam moiety is directed toward the active site dizinc center through the interactions of aminocarbonyl and carboxylate groups with the two active site zinc ions and the two conserved residues, Lys167 and Asn176. From the determination of the potential energy profile of a relevant enzymatic reaction model, it is found that the nucleophilic displacement reaction step proceeds with a low-barrier height, leading to the formation of an energetically favored reaction intermediate. The results also show that the high catalytic activity of the CcrA enzyme stems from a simultaneous operation of three catalytic components: activation of the bridging hydroxide nucleophile by zinc-coordinated Asp86; polarization of the substrate aminocarbonyl group by the first zinc ion; stabilization of the negative charge developed on the departing amide nitrogen by the second zinc ion. Consistent with the previous experimental finding that the proton-transfer reaction step is rate-limiting, the activation energy of the second step is found to be 1.6 kcal/mol higher than that of the first step. Finally, through an examination of the structural and energetic features of binding of a thiazolidinecarboxylic acid inhibitor to the active site dizinc center, a two-step inhibition mechanism involving a protonation-induced ligand exchange reaction is proposed for the inhibitory action of a tight-binding inhibitor possessing a thiol group.

Introduction

It is well-known that bacterial resistance to β-lactam antibiotics stems from the expression of a β-lactamase that catalyzes the hydrolytic cleavage of the substrate amide bond. Of the four structural classes of this enzyme, metallo-β-lactamases (Class B) contain zinc and other divalent cations as cofactors. Although the relative population of the Class B β-lactamases is low, their broad substrate specificity and the absence of clinically useful inhibitors make pathogens with genes encoding this enzyme a hazard to human health. Therefore, a great deal of effort has been devoted to understanding structural and mechanistic properties of metallo-β-lactamases from a variety of bacterial strains including *Bacillus cereus*,[1−3] *Pseudomonas aeruginosa*,[4−6] *Stenotrophomonas maltophilia*,[7,8] *and Aeromonas* hydrophila.[9,10]

In part due to its high activity against most classes of β-lactam antibiotics, the metallo-β-lactamase CcrA from *Bacteroides fragilis*, to date, has been most extensively studied. X-ray crystal structures have been reported for the CcrA enzyme in its resting state.[11,12] The active site includes two zinc ions, both of which are required for full catalytic activity.[13] One zinc ion (Zn1) is liganded with three histidine residues (His82, His84, His145)[14] and a bridging hydroxide ion (Wat1), which is reminiscent of the carbonic anhydrase II active site.[15,16] The second zinc ion (Zn2) has five ligands: an aspartate (Asp86), a cysteine (Cys164), a histidine (His206), apical water (Wat2), and Wat1.

(1) Carfi, A.; Pares, S.; Duee, E.; Galleni, M.; Frere, J.-M.; Dideberg, O. *EMBO J.* **1995**, *14*, 4914−4921.
(2) Carfi, A.; Duee, E.; Galleni, M.; Frere, J.-M.; Dideberg, O. *Acta Crystallogr.* **1998**, *D54*, 313−323.
(3) Fabiane, S. M.; Sohi, M. K.; Wan, T.; Payne, D. J.; Bateson, J. H.; Mitchell, T.; Sutton, B. J. *Biochemistry* **1998**, *37*, 12404−12411.
(4) Concha, N. O.; Janson, C. A.; Rowling, P.; Pearson, S.; Cheever, C. A.; Clarke, B. P.; Lewis, C.; Galleni, M.; Frere, J.-M.; Payne, D. J.; Bateson, J. H.; Abdel-Meguid, S. S. *Biochemistry* **2000**, *39*, 4288−4298.
(5) Toney, J. H.; Hammond, G. G.; Fitzgerald, P. M. D.; Sharma, N.; Balkovec, J. M.; Rouen, G. P.; Olson, S. H.; Hammond, M. L.; Greenlee, M. L.; Gao, Y.-D. *J. Biol. Chem.* **2001**, *276*, 31913−31918.
(6) Oelschlaeger, P.; Schmid, R. D.; Pleiss, J. *Biochemistry* **2003**, *42*, 8945−8956.
(7) Ullah, J. H.; Walsh, T. R.; Taylor, I. A.; Emery, D. C.; Verma, C. S.; Gamblin, S. J.; Spencer, J. *J. Mol. Biol.* **1998**, *284*, 125−136.
(8) McManus-Munoz, S.; Crowder, M. W. *Biochemistry* **1999**, *38*, 1547−1553.
(9) Yang, Y.; Keeney, D.; Tang, X.-J.; Canfield, N.; Rasmussen, B. A. *J. Biol. Chem.* **1999**, *274*, 15706−15711.
(10) Valladares, M. H.; Felici, A.; Weber, G.; Adolph, H. W.; Zeppezauer, M.; Rossolini, G. M.; Amicosante, G.; Frere, J. M.; Galleni, M. *Biochemistry* **1997**, *36*, 11534−11541.
(11) Concha, N. O.; Rasmussen, B. A.; Bush, K.; Herzberg, O. *Structure* **1996**, *4*, 823−836.
(12) Carfi, A.; Duee, E.; Paul-Soto, R.; Galleni, M.; Frere, J.-M.; Dideberg, O. *Acta Crystallogr.* **1998**, *D54*, 47−57.
(13) Crowder, M. W.; Wang, Z.; Franklin, S. L.; Zovinka, E. P.; Benkovic, S. J. *Biochemistry* **1996**, *35*, 12126−12132.
(14) Throughout this paper, we follow a numbering scheme that begins at the amino terminus of the 232-residue mature protein although the sequence of the metallo-β-lactamase from *B. fragilis* contains 249 amino acids.
(15) Eriksson, A. E.; Jones, A. T.; Liljas, A. *Proteins* **1988**, *4*, 274−282.
(16) Håkansson, K.; Carlsson, M.; Svensson, L. A.; Liljas, A. *J. Mol. Biol.* **1992**, *227*, 1192−1204.

10.1021/ja042607b CCC: $30.25

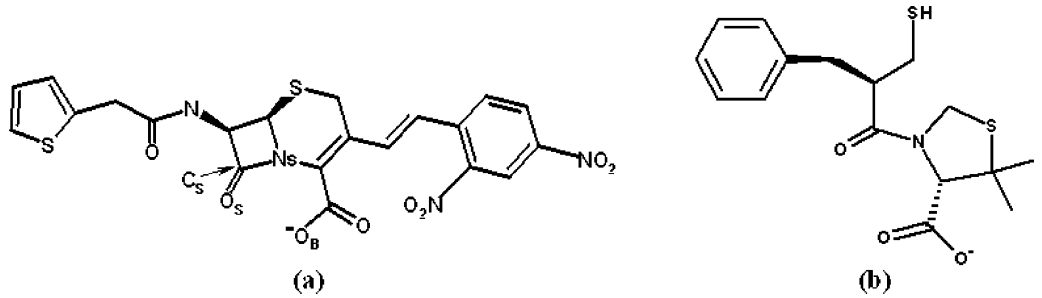

Figure 1. Chemical structures of (a) the substrate nitrocefin with labels for some key atoms on the β-lactam group and (b) the inhibitor morpholineethanesulfonic acid.

Kinetic measurements of mutant enzymes show that changes at the zinc-coordinated amino acid residues lead to impaired catalytic activity.[17−19]

Since the initial discovery of trifluoromethyl alcohol and ketone as lactamase inhibitors,[20] a number of new inhibitors of metallo-β-lactamase have been discovered with significant structural diversity.[21−26] X-ray crystallographic studies have also characterized the structures of the CcrA enzyme complexed with competitive inhibitors, such as 4-morpholineethanesulfonate[27] and biphenyl tetrazole L-159061.[28] Dyson and co-workers compared the dynamic properties of the enzyme in complex with a tight-binding thiazolidinecarboxylic acid (TCA) inhibitor to that of the apoenzyme.[29,30] They showed that although loop structures covering the active site have a greater flexibility than other parts of the enzyme, the motions of these flexible loops are damped out upon binding of the TCA inhibitor. On the basis of this finding, they argued that the broad substrate specificity and tight substrate binding of the CcrA enzyme could be attributed to the malleability of the loop structures. A similar change of the dynamic flexibility was also observed in a molecular dynamics simulation study of the CcrA enzyme in complex with the same inhibitor.[31]

Although a 3-D structure of the enzyme−substrate complex has not been described, the mode of substrate binding to the active site was proposed on the basis of experimental findings. The aminocarbonyl oxygen and nitrogen atoms of the β-lactam ring are believed to interact with Zn1 and Zn2, respectively.[32] A detailed catalytic mechanism has been investigated for hydrolyzing a β-lactam substrate by the CcrA enzyme[32−34] and by dinuclear zinc clusters[35,36] designed as a functional mimic of the enzyme. From these kinetic studies, it appears that the leaving amide moiety is coordinated to the Zn2 site in its deprotonated form. The protonation of the negatively charged intermediate proved to be the rate-limiting step in the catalytic cycle.

Besides the large amount of experimental work, a few theoretical studies on the CcrA enzyme have also been reported to address the coordination structure of active site dizinc center,[37−40] catalytic mechanism,[41,42] and ligand binding.[43,44] In this paper, we address the dynamic properties of the CcrA enzyme bound to nitrocefin (Figure 1) based on hybrid QM/MM molecular dynamics simulations. With the newly developed semiempirical PM3 parameters for the zinc ion in hand,[45] we determined the stable interactions between the enzyme and substrate groups to obtain detailed mechanistic insights.

Following the all-atom simulation, DFT calculations were performed to determine the potential energy profile and the stationary-state structures on the minimum energy path of an enzymatic reaction model. A few years ago, Wang et al. established a minimal kinetic mechanism of the CcrA enzyme that consists of four elementary reaction steps:[32−34]

$$\mathrm{E} + \mathrm{S} \underset{k_{-1}}{\overset{k_1}{\rightleftharpoons}} \mathrm{ES} \xrightarrow{k_2} \mathrm{EI} \xrightarrow{k_3} \mathrm{EP} \underset{k_{-4}}{\overset{k_4}{\rightleftharpoons}} \mathrm{E} + \mathrm{P} \qquad (1)$$

The first and fourth steps correspond to substrate binding and product release, respectively, and they were found to be rapid

(17) Li, Z.; Rasmussen, B. A.; Herzberg, O. *Protein Sci.* **1999**, *8*, 249−252.
(18) Yanchak, M. P.; Taylor, R. A.; Crowder, M. W. *Biochemistry* **2000**, *39*, 11330−11339.
(19) Fast, W.; Wang, Z.; Benkovic, S. J. *Biochemistry* **2001**, *40*, 1640−1650.
(20) Walter, M. W.; Felici, A.; Galleni, M.; Soto, R. P.; Adlington, R. M.; Baldwin, J. E.; Frère, J.-M.; Gololobov, M.; Schofield, C. J. *Bioorg. Med. Chem. Lett.* **1996**, *6*, 2455−2458.
(21) Tsang, W. Y.; Dhanda, A.; Schofield, C. J.; Frère, J.-M.; Galleni, M.; Page, M. I. *Bioorg. Med. Chem. Lett.* **2004**, *14*, 1737−1739.
(22) Buynak, J. D.; Chen, H.; Vogeti, L.; Gadhachanda, V. R.; Buchanan, C. A.; Palzkill, T.; Shaw, R. W.; Spencer, J.; Walsh, T. R. *Bioorg. Med. Chem. Lett.* **2004**, *14*, 1299−1304.
(23) Boerzel, H.; Koeckert, M.; Bu, W.; Spingler, B.; Lippard, S. J. *Inorg. Chem.* **2003**, *42*, 1604−1615.
(24) Siemann, S.; Clarke, A. J.; Viswanatha, T.; Dmitrienko, G. I. *Biochemistry* **2003**, *42*, 1673−1683.
(25) Walter, M. W.; Valladares, M. H.; Adlington, R. M.; Amicosante, G.; Baldwin, J. E.; Frère, J.-M.; Galleni, M.; Rossolini, G. M.; Schofield, C. J. *Bioorg. Chem.* **1999**, *27*, 35−40.
(26) Greenlee, M. L.; Laub, J. B.; Balkovec, J. M.; Hammond, M. L.; Hammond, G. G.; Pompliano, D. L.; Toney, J. H. *Bioorg. Med. Chem. Lett.* **1999**, *9*, 2549−2554.
(27) Fitzgerald, P. M. D.; Wu, J. K.; Toney, J. H. *Biochemistry* **1998**, *37*, 6791−6800.
(28) Toney, J. H.; Fitzgerald, P. M. D.; Grover-Sharma, N.; Olson, S. H.; May, W. J.; Sundelof, J. G.; Vanderwall, D. E.; Cleary, K. A.; Grant, S. K.; Wu, J. K.; Kozarich, J. W.; Pompliano, D. L.; Hammond, G. G. *Chem. Biol.* **1998**, *5*, 185−196.
(29) Scrofani, S. D. B.; Chung, J.; Huntley, J. J. A.; Benkovic, S. J.; Wright, P. E.; Dyson, H. J. *Biochemistry* **1999**, *38*, 14507−14514.
(30) Huntley, J. J. A.; Scrofani, S. D. B.; Osborne, M. J.; Dyson, H. J. *Biochemistry* **2000**, *39*, 13356−13364.
(31) Salsbury, F. R., Jr.; Crowley, M. F.; Brooks, C. L., III. *Proteins* **2001**, *44*, 448−459.
(32) Wang, Z.; Fast, W.; Benkovic, S. J. *Biochemistry* **1999**, *38*, 10013−10023.
(33) Wang, Z.; Benkovic, S. J. *J. Biol. Chem.* **1998**, *273*, 22402−22408.
(34) Wang, Z.; Fast, W.; Benkovic, S. J. *J. Am. Chem. Soc.* **1998**, *120*, 10788−10789.
(35) Kaminskaia, N. V.; Spingler, B.; Lippard, S. J. *J. Am. Chem. Soc.* **2001**, *123*, 6555−6563.
(36) Kaminskaia, N. V.; Spingler, B.; Lippard, S. J. *J. Am. Chem. Soc.* **2000**, *122*, 6411−6422.
(37) Gilson, H. S. R.; Krauss, M. *J. Am. Chem. Soc.* **1999**, *121*, 6984−6989.
(38) Diaz, N.; Suarez, D.; Merz, K. M., Jr. *J. Am. Chem. Soc.* **2000**, *122*, 4197−4208.
(39) Diaz, N.; Suarez, D.; Merz, K. M., Jr. *J. Am. Chem. Soc.* **2001**, *123*, 9867−9879.
(40) Peraro, M. D.; Vila, A. J.; Carloni, P. *Inorg. Chem.* **2003**, *42*, 4245−4247.
(41) Olsen, L.; Antony, J.; Ryde, U.; Adolph, H.-W.; Hemmingsen, L. *J. Phys. Chem. B* **2003**, *107*, 2366−2375.
(42) Olsen, L.; Rasmussen, T.; Hemmingsen, L.; Ryde, U. *J. Phys. Chem. B* **2004**, *108*, 17639−17648.
(43) Oelschlaeger, P.; Schmid, R. D.; Pleiss, J. *Biochemistry* **2003**, *42*, 8945−8956.
(44) Olsen, L.; Pettersson, I.; Hemmingsen, L.; Adolph, H.-W.; Jorgensen, F. S. *J. Comput.-Aided Mol. Des.* **2004**, *18*, 287−302.
(45) Brothers, E. N.; Suarez, D.; Deerfield, D. W., II; Merz, K. M., Jr. *J. Comput. Chem.* **2004**, *25*, 1677−1692.

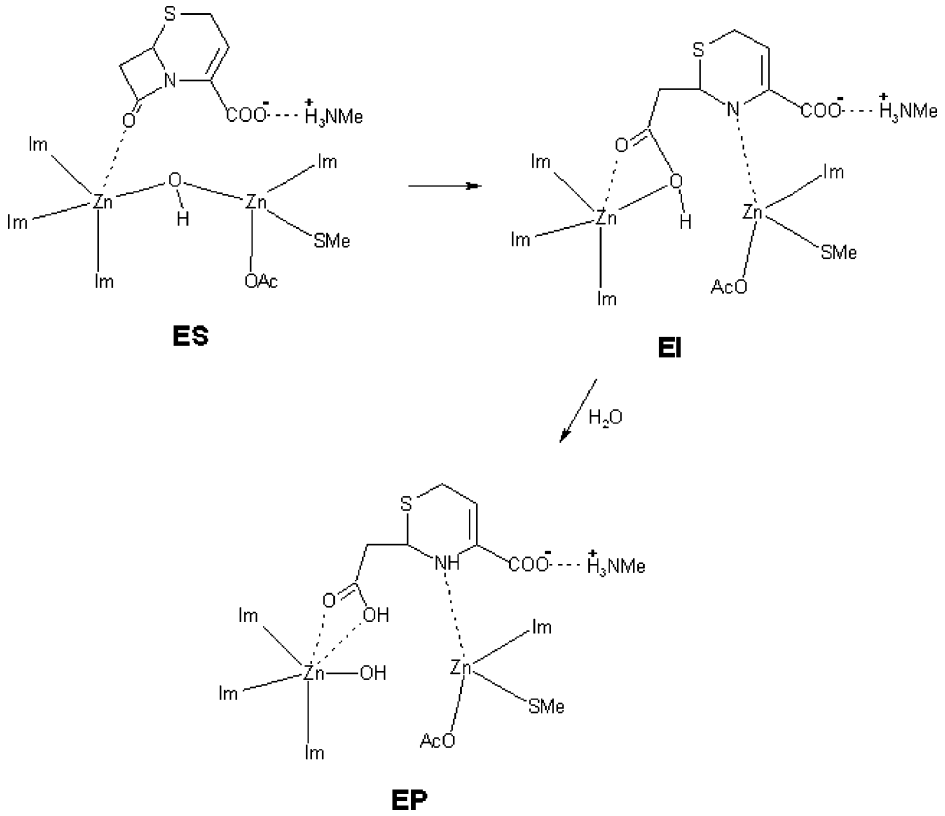

Figure 2. A simplified reaction model of the CcrA enzyme involving the nucleophilic attack of the substrate amide group by the bridging hydroxide ion and the hydrolysis of the reaction intermediate by an external water molecule.

with respect to the remaining two steps. Therefore, we focus our interest on the second and third steps that are characterized by nucleophilic attack of the bridging hydroxide ion on the substrate and protonation of the leaving amine group, respectively. Our model system involves a simplified form of nitrocefin and a hydroxide-bridged dinuclear zinc cluster as depicted in Figure 2. In this model for the enzyme−substrate complex (**ES**) imidazole (Im) molecules, acetate and thiolate ions are used, respectively, to represent four histidine residues, Asp86, and Cys164 coordinated to active site zinc ions while methylammonium ion mimics the active site Lys167 side chain. Based on the computed potential energy profiles for the two reaction steps, we also address the kinetic aspects of the enzymatic hydrolysis of β-lactam antibiotics.

We finally investigate the inhibition mechanism of the CcrA enzyme by the TCA inhibitor, which has a nanomolar inhibitory activity.[46,47] It has been proposed that the sulfur side chain of the inhibitor could be coordinated to the active site zinc ions by displacing the bridging hydroxide ligand.[31] Based on DFT calculations on the model system shown in Figure 3, we address the structural and energetic features of the binding of the TCA inhibitor to the dizinc center of the CcrA enzyme. By calculating the equilibrium structures and energies of model complexes, we have proposed an inhibition mechanism for the active site dizinc center of CcrA by the thiol group.

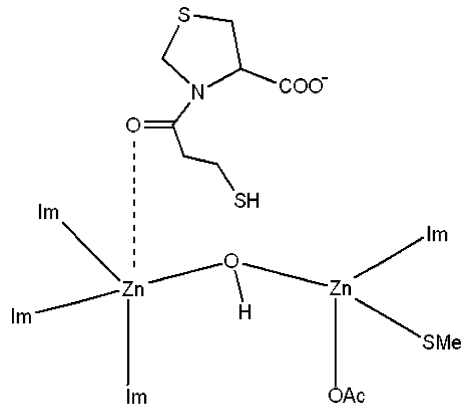

Figure 3. Model system for the dinuclear zinc cluster of the CcrA enzyme in complex with the thiazolidinecarboxylic acid inhibitor. Im designates the imidazole moiety of the histidine side chain.

Computational Methods

QM/MM Simulation of the Enzyme−Nitrocefin Complex. To obtain a starting structure we used the latest version of the AutoDock program.[48] It combines a rapid energy evaluation with various search algorithms to find suitable binding positions for a ligand on a protein receptor. Although the protein structure is fixed, the program allows torsional flexibility of the ligand. Docking of nitrocefin into the active site of CcrA enzyme followed a standard protocol and was carried out using an empirical free energy function with the Lamarckian genetic algorithm.[48] Independent docking runs (200) were carried out for the nitrocefin molecule. Results differing by less than 1.5 Å in positional root-mean-square deviation were clustered together, and the entire cluster was represented by the pose that had the most favorable free

(46) Payne, D. J.; Coleman, K.; Cramp, R. *J. Antimicrob. Chemother.* **1991**, *28*, 775−776.
(47) Payne, D. J.; Cramp, R.; Winstanley, D. J.; Knowles, D. J. *Antimicrob. Agents Chemother.* **1994**, *38*, 767−772.
(48) Morris, G. M.; Goodsell, D. S.; Halliday, R. S.; Huey, R.; Hart, W. E.; Belew, R. K.; Olson, A. J. *J. Comput. Chem.* **1998**, *19*, 1639−1662.

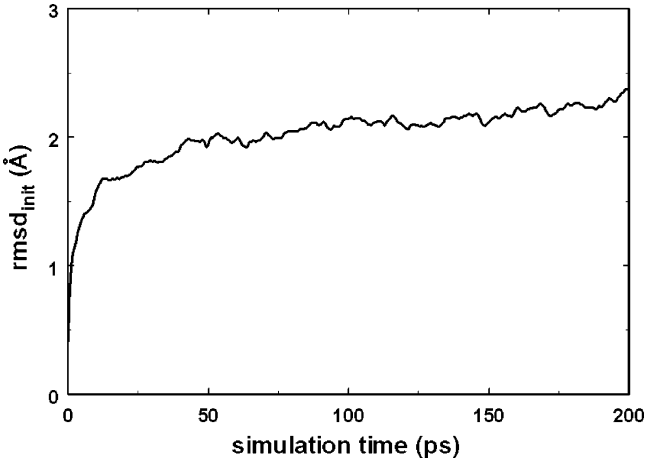

Figure 4. Time dependence of the root-mean-square deviation from the starting structure ($rmsd_{init}$).

energy of binding. The coordinates of the protein atoms were taken from the 1.85 Å crystal structure.[11]

The PM3 semiempirical Hamiltonian was used to describe the side chains of His82, His84, Asp86, His145, Cys164, His206, the two catalytic zinc ions, the bridging hydroxide, the apical water ligand, and the β-lactam moiety of nitrocefin. The semiempirical parameters for the zinc atom used in this study are not the standard PM3 parameters. Due to difficulties with the original parameter set in describing zinc complexes, a reparametrization was undertaken. The new parameters have been optimized versus a diverse set of compounds, including several compounds designed to mimic zinc in biological environments.[45] No other parameters were altered from the original PM3 values. The AMBER force field represented the remainder of the enzyme−substrate complex, and TIP3P water molecules were used to represent the solvent within 20 Å of the nitrocefin molecule. Junctions between the QM and MM regions were made between the CA and CB atoms of the zinc-coordinated residues using the "link atom" approach.[49] Following a 10 ps equilibration run at 298.15 K, a 200 ps production MD simulation was carried out using the ROAR 2.0 program,[50] with residues and solvent molecules within a 20 Å sphere of the substrate being allowed to move.

DFT Calculations. All geometries corresponding to energy minima and transition states on the reaction path were fully optimized with the JAGUAR program.[51] These geometry optimizations were carried out with the 6-31G* basis set for all atoms except for the two zinc ions for which the effective core potential developed by Hay et al. was used.[52] The B3LYP hybrid density functional was employed for all calculations. This functional consists of Becke's hybrid gradient-corrected exchange functional[53] and the gradient-corrected correlation functional of Lee, Yang, and Parr.[54]

Results and Discussion

QM/MM Simulation. As an estimation of the structural stability of the CcrA-nitrocefin complex during the simulation, we calculated the time evolution of the root-mean-square deviation from the starting structure, $rmsd_{init}$. This function describing the fluctuations of all moving heavy atoms is plotted in Figure 4. Overall, the $rmsd_{init}$ values remain between 2 and 2.5 Å, after about 50 ps of equilibration, indicating that a plateau region within the simulation has been reached, though the trend is slightly upward from 50 ps → 200 ps.

Depicted in Figure 5 is a schematic of the key residues interacting with the substrate β-lactam group in a representative MD trajectory snapshot. We see that the substrate is bound in the active site through direct coordination of the substrate aminocarbonyl oxygen (O_S) to Zn1 and hydrogen bond interactions of O_S and the substrate carboxylate oxygen with Asn176 and Lys167, respectively. Interestingly, the apical water ligand (Wat2) is replaced with the substrate carboxylate group, and the bridging hydroxide ion has moved away from Zn2 to situate itself in an orientation suitable for nucleophilic attack on the aminocarbonyl carbon, reinforcing the notion that it is the nucleophile in the catalytic reaction.

To probe the stability of coordination environment of Zn2 in the enzyme−substrate complex, we calculated the time dependence of selected interatomic distances, which are shown in Figure 6. We see that, in the presence of the substrate, the bridging hydroxide (Wat1) moves away from Zn2 and is stabilized at a distance of ∼5 Å from Zn2. Interestingly, the coordination between Zn2 and Wat2 is ruptured upon binding of the nitrocefin substrate, which leads to the transfer of this water molecule to the bulk solvent. This result provides evidence for the mechanistic proposal by Wang and co-workers.[33] The substrate carboxylate oxygen (O_B) forms a bond with Zn2 at a distance of ∼3 Å in the first 30 ps, and this is maintained for the entire simulation, consistent with the spectroscopic characterization of nitrocefin hydrolysis under the catalysis of a dinuclear zinc(II) model cluster for the active site of CcrA enzyme.[35]

The need for a carboxylate group on the substrate in order to afford good affinity is well-known.[55] Earlier docking simulation studies for ampicillin, penicillin, and ceftazidime substrates suggested that it would form a salt bridge with the positively charged side chain of Lys167.[33] Figure 7 shows the variation of the interatomic distance between NZ atom of Lys167 and the nitrocefin O_B atom with simulation time. This distance initially is ∼4 Å and at around 100 ps, and the NZ···O_B drops down to about 2.5 Å. These results indicate that the formation of such a stable hydrogen bond along with the interaction with Zn2 should stabilize the CcrA−nitrocefin complex and place it in a precatalytic orientation through the disruption of the Zn1−OH- - -Zn2 interaction.

It has been proposed that Zn1 and Asn176 would provide an oxyanion hole enhancing the polarization of the β-lactam's aminocarbonyl bond upon substrate binding. As a check on this hypothesis, we calculated the distances from O_S to Zn1 and to the ND2 atom of Asn176. As can be seen in Figure 8, the Zn1···O_S distance is ∼3 Å after about 60 ps, with a time average of 3.01 Å. Similarly, the O_S atom is hydrogen-bonded to Asn167 for 90% of the simulation time when 3.50 Å for the ND2···O_S distance is used as a hydrogen bond cutoff distance. Thus, our simulation provides evidence for the stabilization of the substrate carbonyl moiety by Zn1 and Asn176. It is likely that such interactions are responsible for stabilizing the negative charge developed in the transition states and intermediates during the catalytic reaction.

(49) Field, M. J.; Bash, P. A.; Karplus, M. *J. Comput. Chem.* **1990**, *11*, 700−733.
(50) Cheng, A.; Stanton, R. S.; Vincent, J. J.; van der Vaart, A.; Damodaran, K. V.; Dixon, S. L.; Hartsough, D. S.; Mori, M.; Best, S. A.; Monard, G.; Garcia, M.; Van Zant, L. C.; Merz, K. M., Jr. *ROAR 2.0*; The Pennsylvania State University: 1999.
(51) Ringnalda, M. N. *Jaguar*; Schroedinger Inc.: Portland, OR, 1997
(52) Hay, P. J.; Wadt, W. R. *J. Chem. Phys.* **1985**, *82*, 270−283.
(53) Becke, A. D. *J. Chem. Phys.* **1993**, *98*, 5648−5652.
(54) Lee, C.; Yang, W.; Parr, R. G. *Phys. Rev. B* **1988**, *37*, 785−789.
(55) Laws, A. P.; Page, M. I. *J. Chem. Soc., Perkin Trans.* **1989**, *2*, 1577−1581.

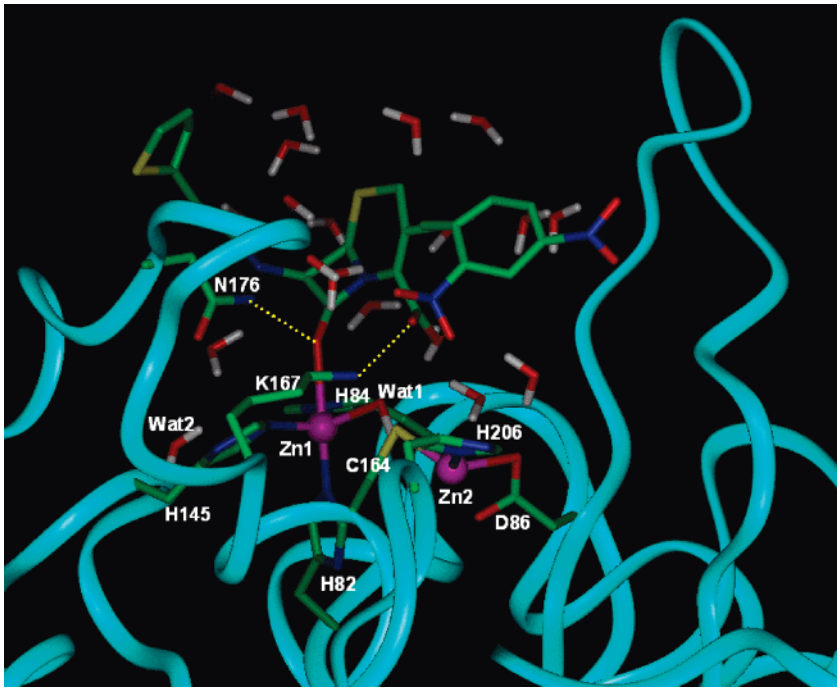

Figure 5. Interactions between the substrate β-lactam group and the enzymatic active site in a representative MD trajectory snapshot for the CcrA−nitrocefin complex. Solvent molecules around the active site are also shown. Hydrogen bond interactions are indicated with yellow dotted lines.

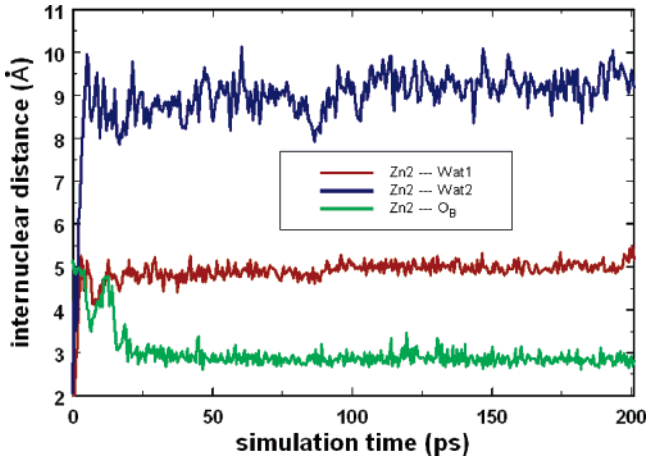

Figure 6. Time evolution of the internuclear distances associated with the Zn2 ion in the CcrA−nitrocefin complex.

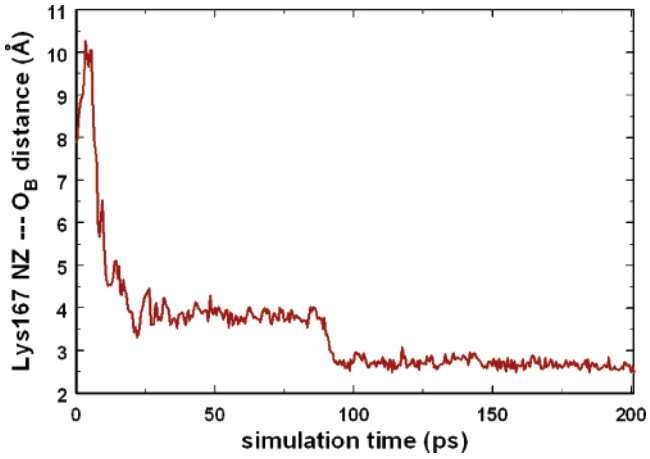

Figure 7. Stabilization of the hydrogen bond between Lys167 and the substrate carboxylate group.

DFT Investigation of the First Catalytic Reaction Step: Nucleophilic Displacement. Although we assume the ionized Asp86 in the preceding QM/MM study based on the previous mechanistic proposals[18,32] and the theoretical evidences,[40] both protonation states are taken into account in the DFT mechanistic study because the possibility of neutral Asp86 has also been proposed.[37,38,56] Thus, we compare the two potential energy profiles for nucleophilic cleavage of a β-lactam C−N bond with varying acid/base forms of acetate in the active site model under consideration. As shown in Figure 9, the activation energy of the nucleophilic substitution with the ionized aspartyl side chain is predicted to be 13.1 kcal/mol lower than that in the neutral Asp86 case. This indicates that the ionized Asp86 would be more effective in catalyzing the first reaction step than the neutral one by a factor of 10^9 using the present active site model.

In the ionized Asp86 case, furthermore, the reaction intermediate (**EI**) is predicted to be 12.8 kcal/mol lower in energy than the reactive complex (**ES**). Such a large energy difference may be sufficient to explain the irreversible formation of an enzyme-bound intermediate in the catalytic action of the CcrA enzyme.[33,34] The 5 kcal/mol instability of **EIH** relative to **ESH** in the neutral Asp86 case may lead to an underestimation of the enzymatic stabilization of the reaction intermediate. Thus, based on this analysis ionized Asp86 is most likely to be both kinetically and thermodynamically favored over the protonated one in the enzymatic reaction within the present active site model and computational level.[40]

The predicted strong dependence of the catalytic activity on the protonation state of Asp86 can be understood by comparing the structural features of the reactive complexes involving ionized (**ES**) and neutral Asp86 (**ESH**). Figure 10 displays the stationary-state structures associated with the first step of the active site model with varying protonation states of Asp86.

(56) Suarez, D.; Brothers, E. N.; Merz, K. M., Jr. *Biochemistry* **2002**, *41*, 6615−6630.

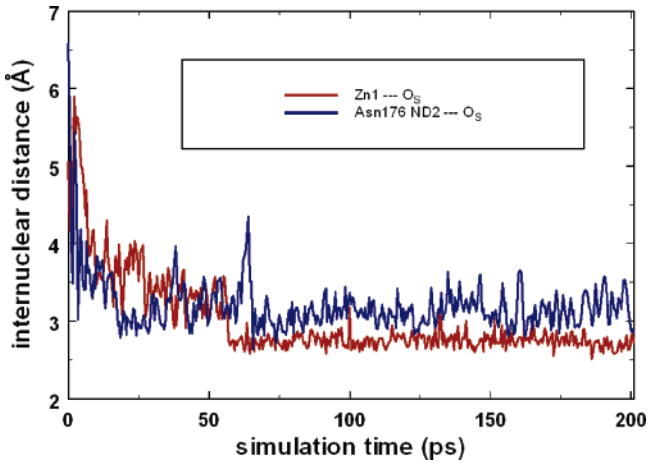

Figure 8. Variation of the interatomic distances from the substrate aminocarbonyl oxygen to Zn1 and to ND2 atom of Asn176 with simulation time.

Consistent with the previous X-ray crystallographic analyses, a strong hydrogen bond is established between Wat1 and Asp86 in both **ES** and **ESH**. It is noteworthy, however, that the change in the protonation state of Asp86 results in switching the roles of donor and acceptor for the two hydrogen-bonding groups. In the structure **ES**, the basicity of Wat1 may increase due to the donation of a hydrogen bond to Asp86, which would in turn have the effect of facilitating its nucleophilic attack upon the substrate aminocarbonyl carbon. Such an activation of the hydroxide nucleophile by Asp86 can be related to the base-catalyzed hydrolysis of an amide bond, which is disfavored under neural conditions. The importance of an active site aspartyl residue as a base catalyst was also observed in the catalytic hydrolysis of a β-lactam substrate by monozinc β-lactamase from *B. cereus*.[41,57] In contrast, the predicted 13.1 kcal/mol rise in the activation energy in the neutral Asp86 case can be attributed to a decreased reactivity of the bridging hydroxide due to the hydrogen-bond stabilization of the nucleophile by the carboxylic acid group. In this regard, the importance of activating the nucleophile has been well appreciated in other theoretical studies of the hydrolysis of the β-lactam ring.[41]

In agreement with previous mechanistic proposals,[18,32] the aminocarbonyl oxygen (O_S) of the model substrate is coordinated to Zn1 at a distance of 2.4 Å in the reactive complex (**ES** in Figure 10). Similar to the role of a Lewis acid catalyst in the amide hydrolysis reaction, such a Zn1···O_S interaction is believed to polarize the substrate carbonyl bond, thereby increasing the susceptibility of substrate aminocarbonyl carbon (C_S) to nucleophilic attack. Due to the O_S coordination to Zn1, the distance between C_S and the Wat1 oxygen (O1) falls to 3.0 Å, a structural feature consistent with the formation of a so-called near attack conformer (NAC).[58] Another important binding force in the **ES** complex is a bidentate hydrogen bond between the carboxylate group of the model substrate and the methylammonium ion, further supporting the proposal of salt bridge formation between the β-lactam substrate and the side chain of Lys167. As mentioned above, the reactivity of the **ES** complex may be enhanced due to a strong hydrogen bond established between O1 and a carboxylate oxygen (OD1) of Asp86 with the interatomic distance of 1.77 Å.

At the reactive complex **ES**, the reaction starts with the approach of O1 to C_S along a line perpendicular to the amide plane of the substrate while the β-lactam C_S-N_S bond is simultaneously weakened. When the O1···C_S distance is reduced to 1.42 Å, the system reaches the first transition state (**ETS1**) in which the Zn1···O_S distance is also contracted to 2.11 Å. In going from **ES** to **ETS1**, the C_S-N_S bond breakage lags behind the C_S···O1 bond formation: the former bond undergoes 0.25 Å stretching, as compared to a 1.61 Å decrease in the C_S···O1 distance. Hence, in the first reaction step the formation of a new C_S···O1 bond and the cleavage of C_S-N_S bond occur in a concerted fashion resembling an S_N2-type reaction. As the reaction proceeds, a new bond path arises between N_S and Zn2, leading to the formation of an interaction at **ETS1** with an associated Zn2···N_S distance of 2.37 Å. On the basis of this observation, it can be argued that the Zn2 ion serves as an electrophilic catalyst in the catalytic cycle, stabilizing the negative charge developed on the leaving amide nitrogen. The decrease of the H1···OD1 distance from 1.77 Å in **ES** to 1.50 Å in **ETS1** implies that a strengthening of the hydrogen bond between the bridging hydroxide and Asp86 is necessary to cross the activation barrier associated with C_S-N_S bond cleavage. The O1$-C_S$ bond formation can be further promoted by breaking the Zn2···Wat1 interaction, which may in turn give rise to a coordination of the substrate carboxylate group to Zn2.

A complete formation of the O1$-C_S$ bond transforms the system into the second energy minimum (**EI**) that corresponds to the enzyme-bound intermediate in the catalytic cycle. In this structure, the amidic C_S-N_S bond is fully broken with the leaving nitrogen atom coordinated to Zn2 in a deprotonated form, confirming the experimental observation of an anionic intermediate bound to a zinc ion in the catalytic reaction of both the *B. fragilis* enzyme[32] and its functional mimic.[36] From **ES** to **EI**, it is worth noting that the proton belonging to Wat1 is fully transferred to OD1. Therefore, it is likely that the nucleophilic cleavage of the substrate amide bond should be accompanied by deprotonation of Wat1 by Asp86 in the enzymatic reaction. This possibility is in line with the mechanistic proposal for the monozinc metallo-β-lactamase from *B. cereus*.[57]

Basically, the catalytic action of the *B. fragilis* enzyme is an amide hydrolysis reaction between a β-lactam substrate and active site groups including zinc ions and the bridging hydroxide ion. It is well-known that the cleavage of an amidic C−N bond in neutral condition is a very slow process, facing an activation barrier of more than 50 kcal/mol.[59,60] However, the reaction can be significantly accelerated by at least three important catalytic factors:[61−63] polarization of the amidic carbonyl group by an acid, activation of a nucleophile by a base, and stabilization of the leaving amine moiety by an electrophilic group. The predicted roles of Zn1, Asp86, and Zn2 in the present study

(57) Bounaga, S.; Laws, A. P.; Gallen, M.; Page, M. I. *Biochem. J.* **1998**, *331*, 703−711.
(58) Bruice, T. C.; Benkovic, S. J. *Biochemisry* **2000**, *39*, 6267−6274.
(59) Oie, T.; Loew, G. H.; Burt, S. K.; Binkley, J. S.; MacElroy, R. D. *J. Am. Chem. Soc.* **1982**, *104*, 6169−6174.
(60) Jensen, J. H.; Baldridge, K. K.; Gordon, M. S. *J. Phys. Chem.* **1992**, *96*, 8340−8351.
(61) Krug, J. P.; Popelier, P. L. A.; Bader, R. F. W. *J. Phys. Chem.* **1992**, *96*, 7604−7616.
(62) Antonczak, S.; Ruiz-López, M. F.; Rivail, J. L. *J. Am. Chem. Soc.* **1994**, *116*, 3912−3921.
(63) Park, H.; Suh, J.; Lee, S. *J. Am. Chem. Soc.* **2000**, *122*, 3901−3908.

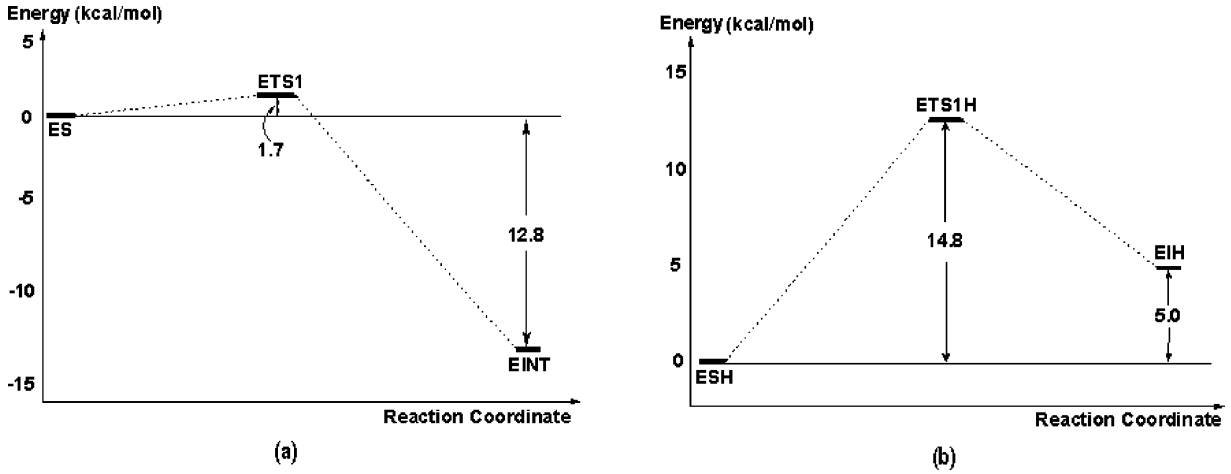

Figure 9. Potential energy profiles for the nucleophilic substitution reaction step of the active site model for the CcrA enzyme with (a) ionized and (b) neutral Asp86.

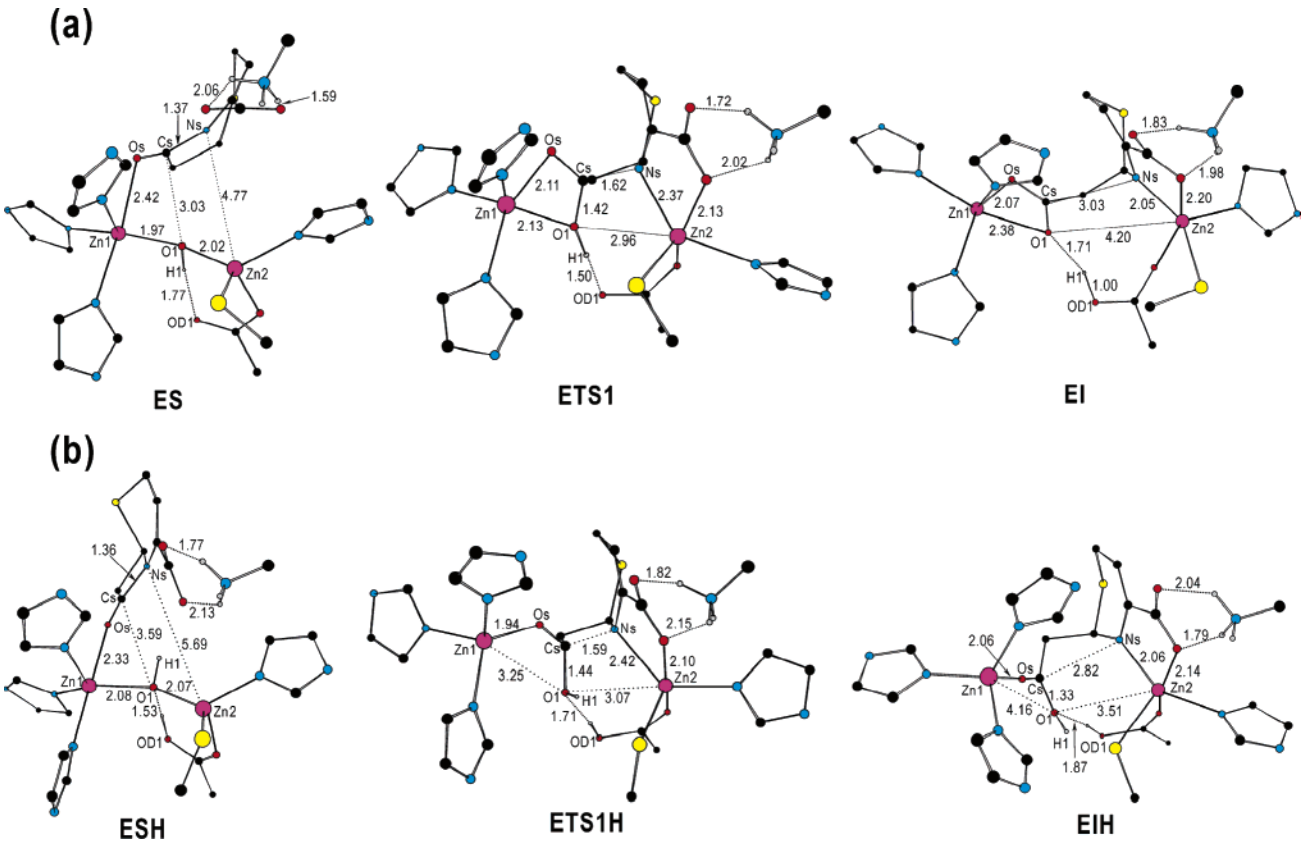

Figure 10. Stationary-state structures encountered along the minimum energy path of the nucleophilic substitution reaction step of the active site model for the CcrA enzyme with (a) ionized and (b) neutral forms of Asp86. For clarity, hydrogen atoms are omitted except for those involved in hydrogen bonds. Selected interatomic distances are indicated in Å.

imply that all three barrier-reducing factors would be involved in the catalytic hydrolysis of a β-lactam substrate by the CcrA enzyme in a cooperative fashion, which may be an explanation for its high catalytic activity.

It is interesting to compare the gas-phase results described here with those obtained from our QM/MM MD simulation on nitrocefin bound to the enzyme. As described above, the QM/MM MD studies suggested that the O1−Zn2 bond is partially broken in ES rather than intact in the optimized structure of the model system at the DFT level of theory. The atomic configuration of ES found in the QM/MM study should facilitate the reaction even further, since it places the nucleophilic oxygen atom O1 in close proximity to C_S and it leads to the binding of N_S to Zn2, which ultimately stabilizes the leaving anion. The DFT **ES** also differs from the corresponding structure found in QM/MM simulation in that the substrate carboxylate group resides distant from Zn2. This may be attributed to the use of a simplified model in the DFT calculations that excludes the macromolecular structure of the CcrA enzyme and solvent effects. Such differences are an example where QM/MM studies provide a different perspective on how the enzymatic reaction might proceed, as compared to the gas-phase DFT studies that can be instructive in energetic features of the enzymatic catalysis.

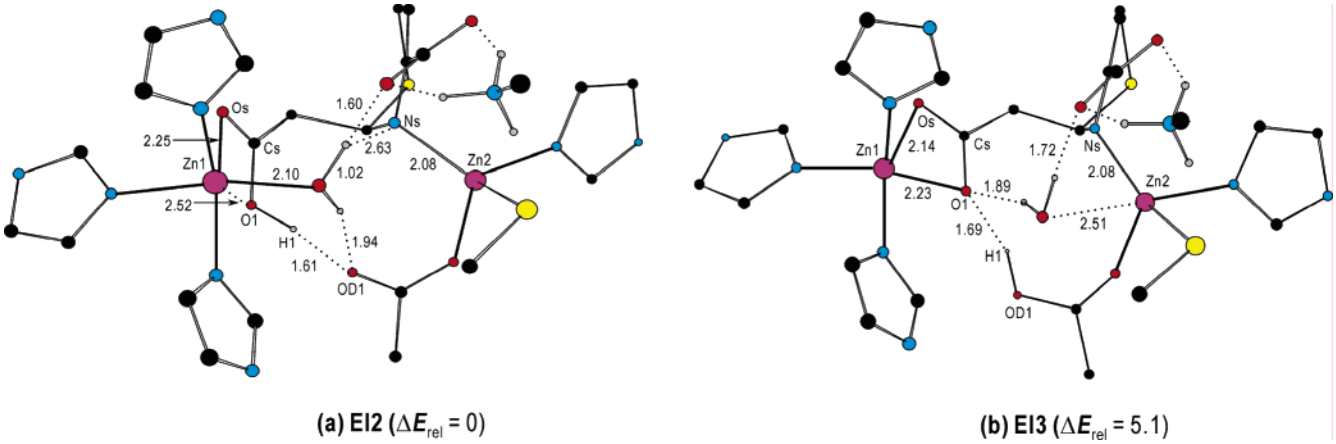

Figure 11. Structures formed by addition of a proton-donating water molecule to (a) Zn1 and (b) Zn2. For clarity, hydrogen atoms are omitted except for those involved in a hydrogen bond. Selected interatomic distances are indicated in Å. Relative energies are also given in kcal/mol.

DFT Investigation of the Second Catalytic Reaction Step: Proton Transfer. This process involves protonating the negatively charged nitrogen coordinated to Zn2 to form the product β-amino acid. It has been speculated that the role of proton donor could be played by a zinc-bound water molecule that originates from bulk solvent.[19,32] Therefore, a preferential zinc site for the coordination of a proton-donating water molecule needs to be identified prior to addressing the energetic and mechanistic features of the proton-transfer step. Figure 11 compares the relative electronic energies (ΔE_{rel}) and structures of the two types of water adducts with **EI**. We find that, at **EI**, Zn1 is predicted to be preferentially hydrated relative to Zn2 (ΔE_{rel} = 5.1 kcal/mol). Therefore, we choose the structure **EI2** as our starting point for the proton-transfer reaction.

As a result of the addition of a water ligand, the O1···Zn1 distance increases from 2.38 Å in **EI** to 2.52 Å in **EI2**, which is accompanied with the proton transfer from OD1 to O1. This implies that Asp86, in its protonated form, may also play a role in product release in the catalytic cycle by protonating the newly formed carboxylate group in the product. Thus, the active site aspartyl residue of the CcrA enzyme is likely to serve as a proton shuttle in the catalytic reaction, similar to the role of Asp90 in the *B. cereus* enzyme.[57] However, it is known that, in the latter case, the Asp residue donates a proton to the leaving amine group. We excluded such a possibility in the present active site model for the CcrA enzyme, following the experimental finding that Asp86 was not observed to be involved in the protonation of the zinc-bound nitrogen leaving group.[18] In **EI2**, the newly added water ligand and Wat1 form hydrogen bonds with OD1 and the substrate carboxylate group at distances of 1.94 Å and 1.60 Å, respectively. Along with these structural changes, the coordinated substrate carboxylate oxygen separates from Zn2.

The potential energy profile for protonating the zinc-bound N_S atom by the new Zn1 water ligand is shown in Figure 12. The activation energy of this second reaction step is found to be 1.6 kcal/mol higher than that of the first step (see also Figure 9), consistent with the previous kinetic data indicating the 10-fold retardation of the proton-transfer step compared to the preceding nucleophilic displacement reaction.[33,34]

At **EI2**, the second catalytic step proceeds with the approach of a hydrogen belonging to the new water ligand to the negatively charged nitrogen (N_S) atom coordinated to Zn2. The structures of the transition state (**ETS2**) and product (**EP**) of

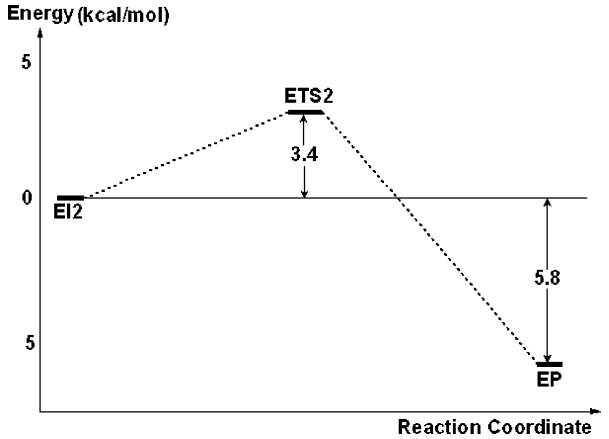

Figure 12. Potential energy profile for the proton-transfer reaction step of enzymatic reaction model.

the proton-transfer reaction are shown Figure 13. As **EI2** moves along the reaction coordinate to form **ETS2**, the H···N_S distance is reduced from 2.63 Å to 1.34 Å, together with the stretching of the donor O−H bond from 1.02 Å to 1.20 Å. Due to this partial deprotonation, the proton-donating water ligand is more tightly coordinated to Zn1, leading to a weakening of the interaction between Zn1 and the carboxylic acid group of the forming product. These structural changes, in turn, bring about a 0.14 Å increase in the OD1···H1 hydrogen bond distance. Simultaneously, the negatively charged nitrogen (N_S) was coordinated to Zn2 in **ETS2** with the associated Zn2···N_S distance 0.09 Å longer than that observed in **EI2**, which results from a partial loss of the negative charge on N_S. Overall, it is apparent that the forming product is capable of disassociating from the active site as **ETS2** moves along the reaction coordinate to **EP**.

Passing through the second transition state, the reacting system falls into the final energy minimum (**EP** in Figure 13) corresponding to the enzymatic dinuclear zinc cluster in complex with the product β-amino acid. Due to the loss of a proton, the Zn1 coordination of the new water ligand gets even stronger, which prohibits the close contact of the product carboxylic acid group to Zn1. Thus, the proton transfer reaction occurs in such a way that it can induce the restoration of a tetrahedral coordination at Zn1 found in the resting state. Despite being fully protonated, however, the product N_S atom is coordinated

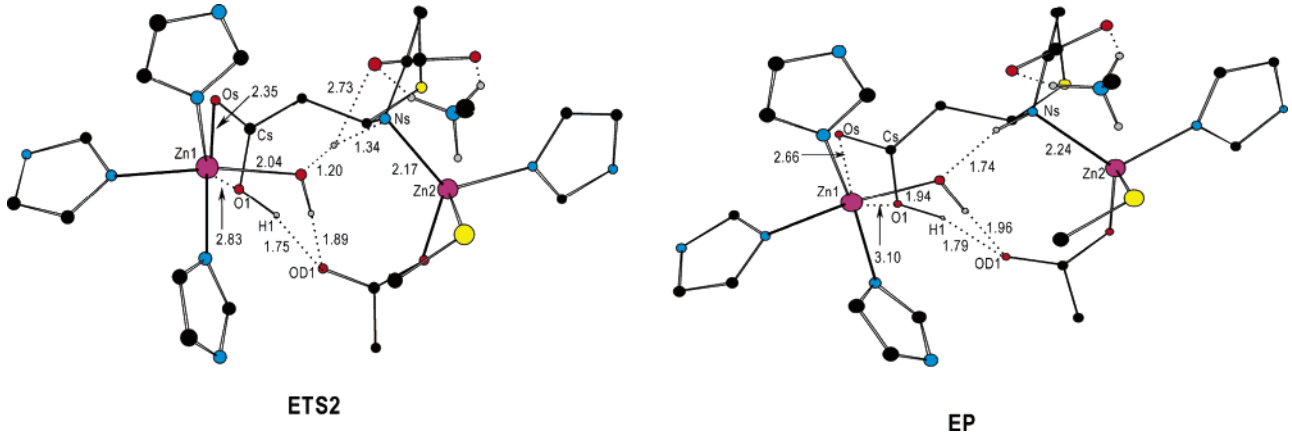

Figure 13. Structures of the transition state and product in the proton-transfer reaction step of an enzyme active site model for the CcrA enzyme. For clarity, the hydrogen atoms have been omitted except for those involved in a hydrogen bond. Selected interatomic distances are indicated in Å.

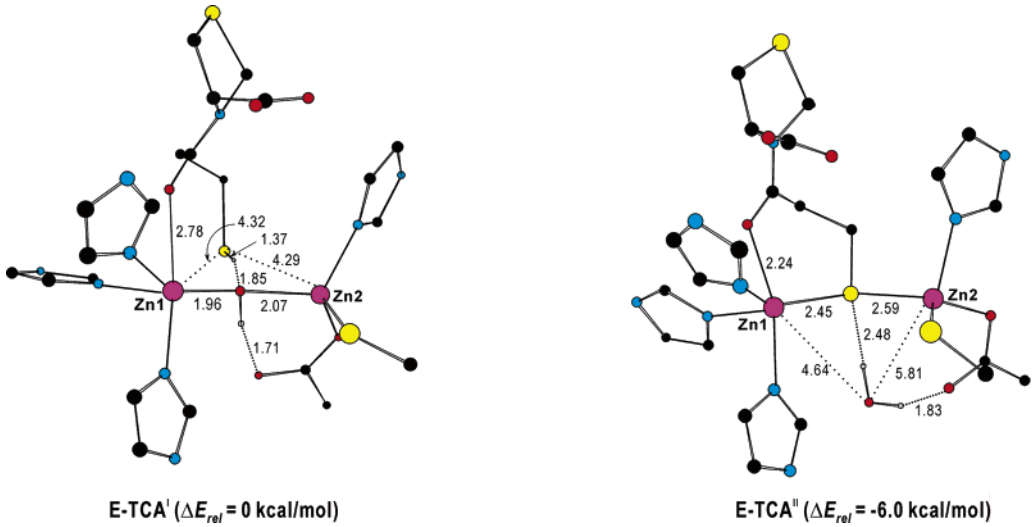

Figure 14. Optimized structures of model zinc complexes representing two binding modes of TCA inhibitor to the active-site dizinc center. For clarity, hydrogen atoms are omitted except for those of Wat1 and the inhibitor thiol group. Selected interatomic distances are indicated in Å.

to Zn2 at a distance of 2.24 Å. This is in strong contrast with the structural feature of the **ES** complex that lacks a significant Zn2···N_S interaction (see Figure 10). Such a difference in zinc affinity is consistent with a difference in basicity between the sp^2 nitrogen in an amide group and the sp^3 nitrogen found in the amine counterpart. In contrast to the maintenance of Zn2···Ns coordination in going from **ETS2** to **EP**, Zn1···O1 and Zn1···O_S interactions get weaker by 0.31 Å and 0.27 Å, respectively, facilitating the separation of the forming β-amino acid from the active site dizinc cluster.

Inactivation of the CcrA Enzyme by a TCA Inhibitor. While it is interesting to understand how CcrA works on a β-lactam substrate, we are also very interested in understanding how known inhibitors inactivate the enzyme. Therefore, we address the structural and energetic features in the inhibition mechanism by a TCA inhibitor that has been used as a structural scaffold for further development of new antibiotics.[22] Shown in Figure 14 are the structures of energy minima that may serve as binding modes of a TCA inhibitor to the dizinc cluster, together with their relative energies (ΔE_{rel}). The first optimized model complex (**E_TCA^{I}**) corresponds to the initial enzyme−inhibitor complex in which the aminocarbonyl oxygen is weakly coordinated to Zn1 at a distance of 2.78 Å. Interestingly, the thiol group of the inhibitor donates a hydrogen bond to the bridging Wat1 ligand with an associated O···H distance of 1.85 Å. Judging from the moderate strength of the hydrogen bond in **E_TCA^{I}** and a relatively weak Zn1···O coordination mode, it can be surmised that we have an inadequate explanation of the tight binding observed for TCA with a nanomolar inhibitory activity.

The proton transfer from the inhibitor thiol group to Wat1 in **E_TCA^{I}** leads to the formation of second energy minimum (**E_TCA^{II}** in Figure 14) in which the Zn1···O coordination bond is established in a stronger form than that in **E_TCA^{I}** with an associated interatomic distance of 2.24 Å. As a consequence of the proton transfer, more importantly, the deprotonated sulfur side chain of the inhibitor bridges the two zinc ions, replacing the Wat1 ligand. Since the potential energy of **E_TCA^{II}** is found to be 6.0 kcal/mol lower than that of **E_TCA^{I}**, the former is believed to be more favorable than the latter in forming a stable enzyme−inhibitor complex. In this regard, the binding mode involving a substitution of the bridging hydroxide ligand was found in the X-ray crystal structures of the IMP-1 dizinc metallo-β-lactamase from *P. aeruginosa* bound to mercaptocarboxylate[4] and succinate[5] inhibitors. The dynamic stability of such a binding mode has also been confirmed in the MD simulation study of the CcrA enzyme in complex with a TCA inhibitor.[31]

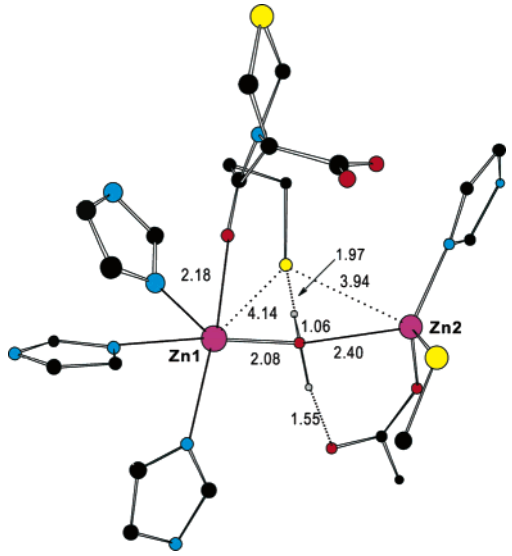

Figure 15. Transition state of the protonation-induced ligand exchange reaction between a TCA inhibitor and the active-site dizinc center. Selected interatomic distances are indicated in Å.

To estimate the activation energy (E_a) and obtain further mechanistic insights, we have also optimized the transition state connecting **E_TCA^{I}** and **E_TCA^{II}**, which is shown in Figure 15. The E_a between the two energy minima is predicted to be 7.5 kcal/mol. As can be inferred from the small changes that occur in the Zn1···S and Zn2···S distances (4.32 Å and 4.29 Å in **E_TCA^{I}** to 4.14 Å and 3.94 Å in the TS), the transition state is early in terms of the ligand exchange. On the other hand, the proton transfer from the inhibitor thiol group to Wat1 is well advanced in the transition state with a contraction of the associated O···H distance from 1.85 Å to 1.06 Å, which corresponds to 91% progress toward the formation of **E_TCA^{II}**. This structural feature of the TS confirms that the protonation of Wat1 is an essential step in crossing the activation barrier.

On the basis of the above structural and energetic results, we propose a two-step reaction mechanism in relation to the tight binding of a TCA inhibitor to the dizinc center of CcrA enzyme as follows:

$$E + I \rightleftarrows EI \rightleftarrows EI^*$$

Here, the first reaction step represents the initial binding of a TCA inhibitor to the enzyme active site, leading to the formation of a precursor-state complex (**EI**) in which the interactions between the inhibitor and dizinc center are presumably similar to those in **E_TCA^{I}**. The final enzyme−inhibitor complex (**EI***) can be formed in the second step through the protonation-induced ligand exchange reaction. As seen in the structure **E_TCA^{II}**, the sulfur side chain of the inhibitor should bridge the active-site zinc ions through strong electrostatic interactions.

Conclusion

Hybrid QM/MM simulation of the metallo-β-lactamase CcrA from *B. fragilis* in complex with nitrocefin shows that the substrate β-lactam group interacts with active site zinc ions, replacing the apical water molecule upon formation of the Michaelis complex. Two conserved residues, Lys167 and Asn176, are found to act as an oxyanion hole for the aminocarbonyl moiety and form a salt bridge with the substrate carboxylate group, respectively. The energetic and mechanistic features of an active site model indicate that the two zinc ions and the active site aspartyl residue (Asp86) should play a significant role in catalysis. The active site zinc ion with tetrahedral coordination (Zn1) provides a binding site for the substrate aminocarbonyl oxygen, rendering the carbon atom more susceptible to nucleophilic attack. The stabilization of the leaving amine group via an electrophilic catalyst in the guise of the second zinc ion is also found to be important in crossing the activation barrier for cleavage of the amide C−N bond. Similar to the role of a base catalyst in solution phase amide hydrolysis, Asp86 can facilitate the cleavage of the substrate C−N bond by deprotonating the bridging hydroxide nucleophile. Consistent with the available kinetic data, the activation energy of the proton-transfer step is predicted to be 1.6 kcal/mol higher than that of the preceding nucleophilic displacement reaction step. The structural and energetic features of the binding of a thiazolidinecarboxylic acid inhibitor show that a thiol group can deactivate the dinuclear zinc center through a two-step reaction mechanism involving the protonation-induced ligand exchange process, leading to the replacement of a bridging Wat1 ligand with the sulfur side chain of the inhibitor.

Acknowledgment. We thank the NIH (GM 44974) for generous support of this work.

JA042607B